Research Square

Preprints are preliminary reports that have not undergone peer review.
They should not be considered conclusive, used to inform clinical practice,
or referenced by the media as validated information.

Operational system based on tide gauge network predicts extreme flooding events for coastal community

Marcelo Di Lello Jordão

dilello@oceanica.ufrj.br

Federal University of Rio de Janeiro (UFRJ)

Eloi Melo

Federal University of Rio Grande (FURG)

Rodrigo Morais Marques Hoerner

Federal University of Rio de Janeiro (UFRJ)

Lucas de Oliveira

Federal University of Rio de Janeiro (UFRJ)

Marcos Nicolas Gallo

Federal University of Rio de Janeiro (UFRJ)

Susana Beatriz Vinzon

Federal University of Rio de Janeiro (UFRJ)

Article

Keywords: Coastal Flooding, Non-Astronomical Tide, Early Warning System, Tide Gauge Network, Statistical Propagation Model.

Posted Date: November 12th, 2026

DOI: https://doi.org/10.21203/rs.3.rs-11363116/v1

License: This work is licensed under a Creative Commons Attribution 4.0 International License.
Read Full License

Additional Declarations: No competing interests reported.

Operational system based on tide gauge network predicts extreme flooding events for coastal community

Abstract

Coastal flooding induced by non-astronomical tides represents a recurrent hazard for vulnerable communities along the Southeast Brazilian coast. The typical models used for this type of prediction have a high computational cost and input data requirements. The regional public models consider only the astronomical tide and the state of the local sea. This study presents the development, validation, and operational application of a low-cost and freely accessible Coastal Flood Forecasting and Early Warning System based on Meteorological Tide (COFFEWS-MT), providing up to 26 hours of lead time for a vulnerable community located in Guanabara Bay, Rio de Janeiro, Brazil. The system is based on a statistical propagation model, which exploits the sub-inertial northward propagation of meteorological tide along the continental shelf. Near real-time sea level data from the Porto de Imbituba gauge station, located 800 km south of Rio de Janeiro, are decomposed into astronomical tide, seasonal, and meteorological components using harmonic analysis and FFT-based filtering. The meteorological tide is propagated to the Ilha Fiscal gauge station through a lagged linear correlation model. Reanalysis for 2022 showed good agreement between predicted and observed sea level, with RMSE of 0.06 m and R^2 of 0.97, significantly outperforming predictions based solely on astronomical tide. Flood and extreme flood thresholds were empirically calibrated using field surveys and historical records. The system operates on minimal hardware and relies on open-access PSMSL/GLOSS data, contributing to UN Decade Challenge 6 by strengthening people-centered coastal flood early warning.

Keywords: Coastal Flooding, Non-Astronomical Tide, Early Warning System, Tide Gauge Network, Statistical Propagation Model.

Author information

- Marcelo D. L. Jordão*[1]
- Eloi Melo Filho[2]
- Rodrigo M.M. Hoerner[1]
- Lucas Olivera[3]
- Marcos N. Gallo[1]
- Susana B. Vinzon[1,3]

[1]Coastal and Oceanographic Engineering Area (AECO), Ocean Engineering Program/COPPE, Federal University of Rio de Janeiro (UFRJ), Rio de Janeiro, 21945-970, Brazil

[2]School of Engineering, Federal University of Rio Grande (FURG), Rio Grande, 96203-000, Brazil.

[3]Departament of Water Resources and Environment (Drhima), Polytechnic School, Federal University of Rio de Janeiro (UFRJ), Rio de Janeiro, 21945-970, Brazil.

*Corresponding author: dilello@oceanica.ufrj.br

1. Introduction

In 2020, almost 11% of the global population (896 million people) lived in the coastal zone below 10 m of elevation above sea level and hydrologically connected to the sea (Low-Elevation Coastal Zone – LECZ)[1], which is expected to potentially exceed 1 billion by 2050[2,3]. These areas are especially vulnerable to coastal flooding events caused by wave set-up, storm surges, and meteorological tides[4,5]. Coastal flooding exceeding the mean higher-high water (MHHW) level often takes vulnerable communities and responsible authorities by surprise, particularly when the underlying drivers are not captured by conventional predictive models. These models typically account only for astronomical tides and sea-state variability associated with swell or locally generated wind waves. Such limitations are evident in coastal flooding events in Rio de Janeiro, which are driven by remote meteorological tides.

The term *"meteorological tide"* is rarely used in the international scientific literature, although it is commonly employed in the Portuguese language. In Brazil, the term *meteorological tide* has been defined either as a synonym for *storm surge*[6] or as the residual signal obtained from harmonic tidal analysis[7]. However, the literature has shown multiple definitions of *storm surge*.

The earliest concept defines storm surge as any sea-level disturbance produced by meteorological forcing, with time scales ranging from a few hours to several days[6,8,9]. Other studies describe storm surge as synonymous with wind set-up or set-down, in which coastal flooding is induced by onshore winds acting at supra-inertial time scales (from 2 hours to 3 days)[4,10,11]. For storm surges induced by geostrophic winds acting at sub-inertial time scales, Dean and Dalrymple[10] adopted the term *bathystrophic storm tides*, originally defined by Freeman[12].

More recently, in a comprehensive review by Woodworth et al.[13], coastal flooding processes were classified according to their dominant mechanisms, distinguishing flooding induced by the propagation of coastally trapped waves[14,15] from storm surge–type flooding, driven by the combined effects of atmospheric pressure (inverse barometer effect) and local geostrophic winds[9,16,17].

According to the concept formalized by Melo[4], a meteorological tide (MT) is defined as non-astronomical sea-level fluctuations with periodicities ranging between 3 and 30 days, a time scale over which Coriolis effects become significant (the sub-inertial period).

These fluctuations reach Rio de Janeiro as a type of long wave, remotely generated by southerly winds blowing parallel to the coast and associated with extratropical cyclones forming between southern Brazil and Argentina[4,18]. When these long waves coincide with spring high tides, flooding of vulnerable coastal communities is recorded. Such flooding often occurs during the early morning hours, catching residents by surprise and resulting in substantial material losses. In communities surrounded by polluted waters, the situation is further aggravated by the risk of contamination.

Until the present study, the coastal communities of the State of Rio de Janeiro had no access to a free forecasting and warning system for flooding associated with meteorological tides and relied solely on astronomical tide tables published annually by the Directorate of Hydrography and Navigation (DHN) of the Brazilian Navy. The meteorological tide predictive models available to date required high implementation and maintenance costs. Among the most widely used approaches are traditional numerical hydrodynamic models and statistical models based on neural networks.

Within the numerical modeling approach applied to southeastern Brazil, the pioneering work of Stech and Lorenzzetti[19] stands out, employing a proprietary numerical model, followed by the development of an operational meteorological tide forecasting system based on the Princeton Ocean Model (POM)[20,21]. França[22] and Freitas et al.[23] demonstrated, using the Hybrid Coordinate Ocean Model (HYCOM), the potential of this model for meteorological tide forecasting. A similar approach was applied in the Río de la Plata region, where a two-dimensional hydrodynamic model (MOHID) with nested domains was used to simulate regional circulation. The model was forced by a mesoscale atmospheric model (WRF) and a global tidal model (FES2004)[24].

Within the statistical approach, the earliest contributions were made by Truccolo[25] and Truccolo et al.[26], who developed a meteorological tide forecasting model for the São Francisco do Sul region, Santa Catarina State (Brazil), based on atmospheric pressure and wind data. Their methodology relied on lagged cross-correlation techniques combined with multiple linear regression models applied in both the time and frequency domains. Models based on Artificial Neural Networks were also applied to the regions of Paranaguá, Paraná State (Brazil)[27–29], Cananéia, São Paulo State (Brazil), and Ponta da Armação, Rio de Janeiro State (Brazil)[30]. Both numerical and statistical approaches proved capable of forecasting meteorological tides, however, none of these systems made their forecasts freely available to the public, particularly to vulnerable communities.

In this context, the present study introduces a free and accessible coastal flooding forecasting and warning system with a 26-hour lead time for vulnerable communities in Rio de Janeiro. The system is based on a statistical model proposed by Melo[4] and was tested and validated through the monitoring of a vulnerable community frequently affected by meteorological tide–induced flooding, located in Guanabara Bay, Rio de Janeiro (RJ), Brazil.

1.1. The meteorological tide in Rio de Janeiro

In the concept formalized by Melo[4], the meteorological tide is a geostrophic phenomenon and therefore depends on Earth's rotation. This implies that the processes generating meteorological tides must operate at time scales longer than the local inertial period. Sea level changes, which are part of the Meteorological Tide, can be linked to three types of waves[31, p. 409]: Kelvin Waves – when the shelf has a constant depth, infinite width, and is bordered by a vertical wall; Continental Shelf Waves – when the shelf has a sloping bottom and homogeneous waters; and Coastally Trapped Waves – when the shelf has a sloping bottom and stratified waters.

Spectral density analysis of non-astronomical sea-level signals recorded by tide gauges located between Rio Grande – RS and Rio de Janeiro - RJ showed that meteorological tides correspond to the sub-inertial band between 3 and 30 days (Table 1). In that study, the sub-inertial period band associated with meteorological tides accounted for approximately 65–80% of the energy distribution of the non-astronomical sea-level signal measured along this stretch of the Brazilian coast.

tides	wave period band
storm tide	2 hours to 3 days
meteorological tide	3 days to 30 days
sazonal tide	30 days to 1 year

Table 1: Classification of non-astronomical tides according to Melo[4]

At the time scales associated with meteorological tides, the atmosphere can induce sea-level variability through the normal stress exerted by atmospheric pressure on the ocean surface and through the tangential stress imposed by wind forcing[4,13]. The effect of atmospheric pressure on ocean waters is known as the inverse barometer (IB) effect, which essentially represents a static oceanic response to the weight of the atmosphere[32]. However, Hamon[33,34] and Hamon and Hannan[35] observed that daily mean sea-level fluctuations along the Australian coast are not primarily barometric in nature.

This result is not physically surprising, as vorticity is a dominant characteristic of continental shelf waves, and pressure fluctuations alone are not expected to be an efficient mechanism for generating vorticity[36]. Continental shelf waves are nondispersive, rotational waves forced by geostrophic winds and propagate cyclonically (counterclockwise) in the Southern Hemisphere[37]. Wind-forced continental shelf waves constitute the primary mechanism responsible for the remote propagation of meteorological tides toward Rio de Janeiro[4,23,38]. Castro and Lee[18] and Filippo et al.[38] also identified free continental shelf waves with periods ranging from 6 to 12 days along the southeastern Brazilian shelf.

Along the Brazilian coast, extratropical cyclones are the primary drivers sustaining winds over the continental shelf and parallel to the coastline on sub-inertial time scales. Figure 1 schematically illustrates the formation and propagation of meteorological tides toward the city of Rio de Janeiro. The process begins with the approach of an extratropical cyclone near the coast. Long-term studies, such as those by Gan and Rao[39], Gramcianinov et al.[40], and Destéfani et al.[41], have shown that the highest frequency of extratropical cyclogenesis occurs between the austral autumn (March–May) and winter (June–August) seasons.

Based on observations from 1979 to 1988, Gan and Rao[39] identified May as the month with the highest cyclone occurrence (139 events) and December as the month with the lowest occurrence (71 events). Using 41 years of data (1979–2019), Gramcianinov et al.[40] and Destéfani et al.[41] identified at least two major regions of extratropical cyclone formation in the South Atlantic: one near the mouth of the Río de la Plata, between latitudes 30° and 40° S, and another in the Gulf of San Matías, between latitudes 40° and 55° S.

Using fifth-generation ECMWF reanalysis wind data for the period from January 1979 to December 2020, Jantsch[42] showed that winds associated with storm surges generated by extratropical cyclones along the coast of Rio Grande do Sul (RS) ranged from 12.1 m s^{-1} to 25.2 m s^{-1}.

When an extratropical cyclone persists along the coast for a duration longer than the local inertial period, southerly winds induce Ekman transport toward the coast, resulting in a local coastal sea-level rise (positive meteorological tide)[4]. Considering the South American coastline, cyclones must persist over the continental shelf for at least one

inertial period of approximately 14.6 h at 55° S (Gulf of San Matías) and 23.9 h at 30° S (Río de la Plata). During this sub-inertial forcing, the coastal sea-level rise evolves into a bulge that necessarily propagates northward in the form of a continental shelf wave (CSW).

The mean propagation speed of CSWs associated with meteorological tides typically ranges between 7.5 m/s and 10 m/s[4,38]. Melo[4] estimated that if a meteorological tide signal is generated along the coast of Rio Grande do Sul (RS), the corresponding CSW would take approximately 51 h to reach Rio de Janeiro (~1425 km). From an even more remote source region, the CSW would require about 77 h to propagate 3010 km from Puerto Madryn, Argentina, to Ilha Fiscal, Rio de Janeiro, Brazil[38].

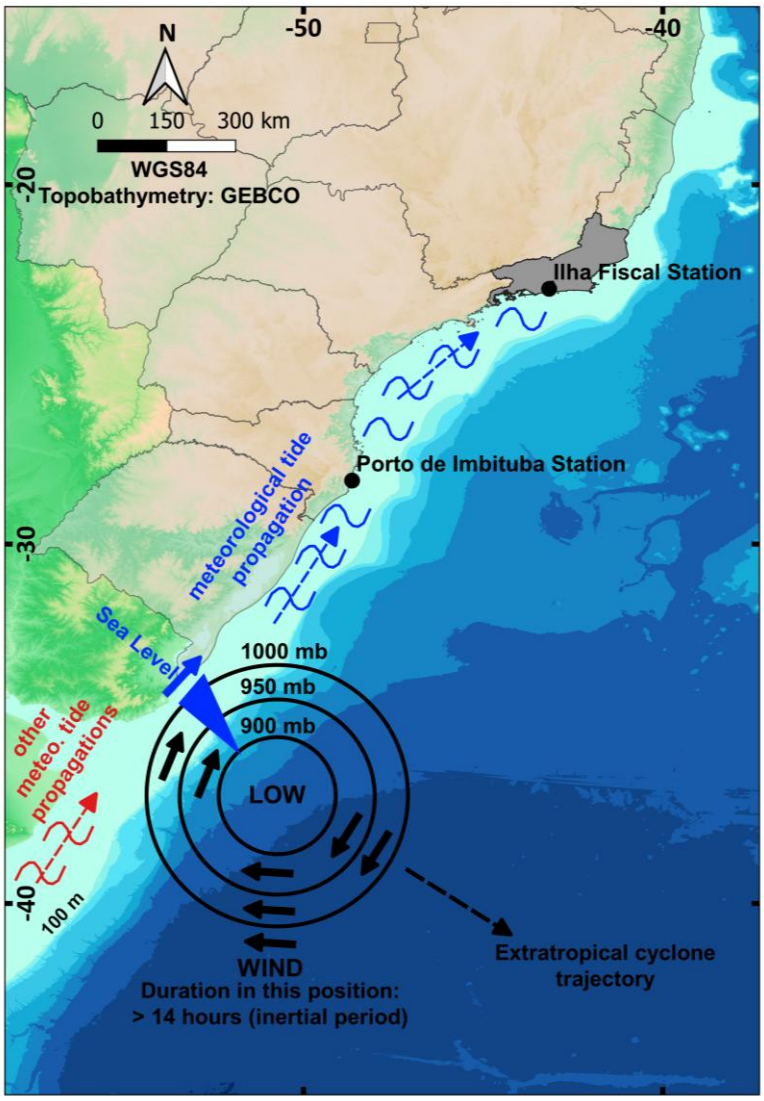


Figure 1: Schematic description of the formation and propagation of the meteorological tide for Rio de Janeiro

2. Materials and methods

2.1. Study area

Vila Residencial is located on Ilha do Fundão, within Guanabara Bay, in the state of Rio de Janeiro, Brazil (Figure 2). The community originated as a small workers' village during the construction of the Rio–Niterói Bridge (1969–1974) and, according to a 2016 estimate, was home to more than 2,000 residents[43]. During the monitoring of flooding events associated with meteorological tides, the most affected streets were Margaridas, Cravos, and Açucenas Streets ("flood warning"). However, historical records provided by the residents themselves indicate that during extreme meteorological tide events, flooding reached nearly the entire community, inundating many houses ("extreme flood warning").

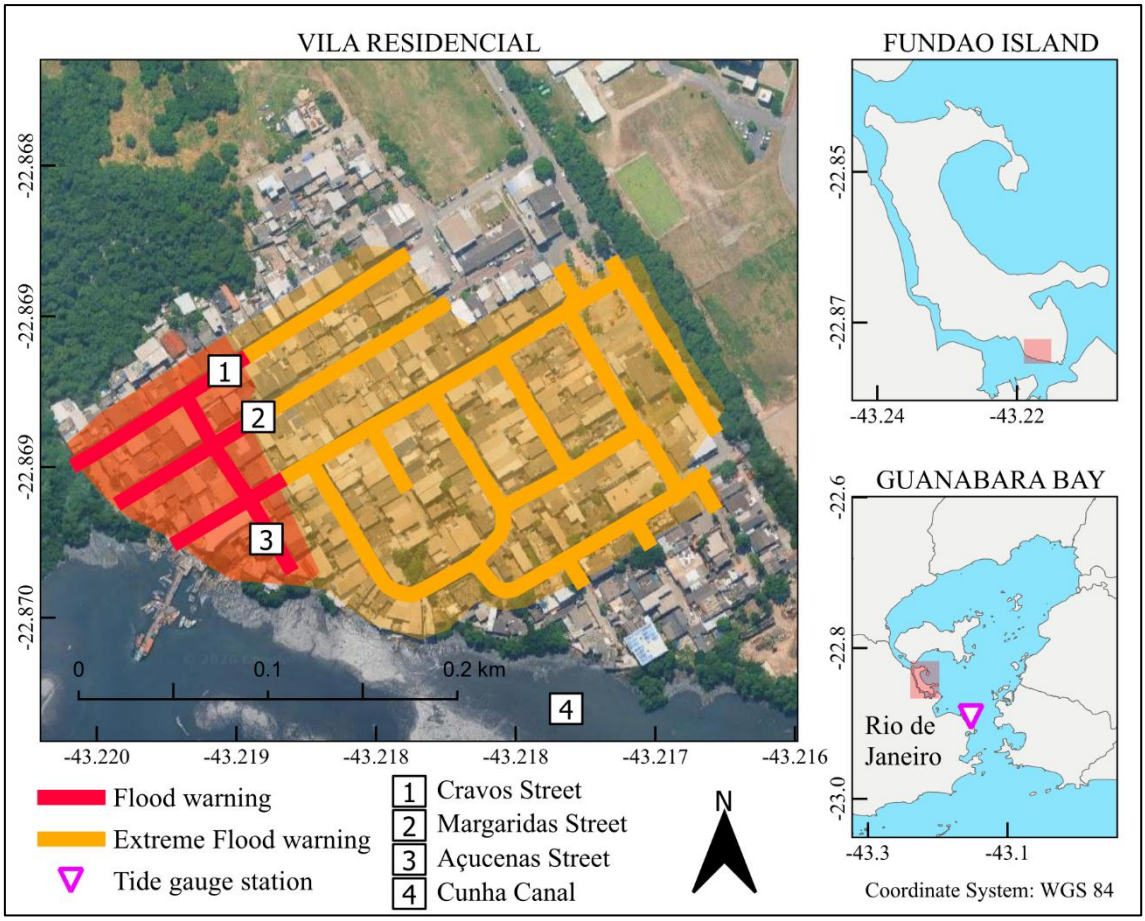


Figure 2: Study area, where the orange zone indicates flood warning and the red zone indicates extreme flood risk based on historical photographs (1963–2021). Fiscal Island Tide Gauge (Lat: -22.89667°, Lon: -43.16592°)

2.2. Meteorological Tide Forecast Model

The hardware consists solely of a Raspberry Pi 4 single-board computer connected to the internet (Figure 3). The algorithm is written in Python™ and runs on the Ubuntu Linux

operating system, using the open-source data science platform Anaconda®. Both the operating system and software environment are configured for the ARM 64-bit architecture of the Raspberry Pi 4 single-board computer.

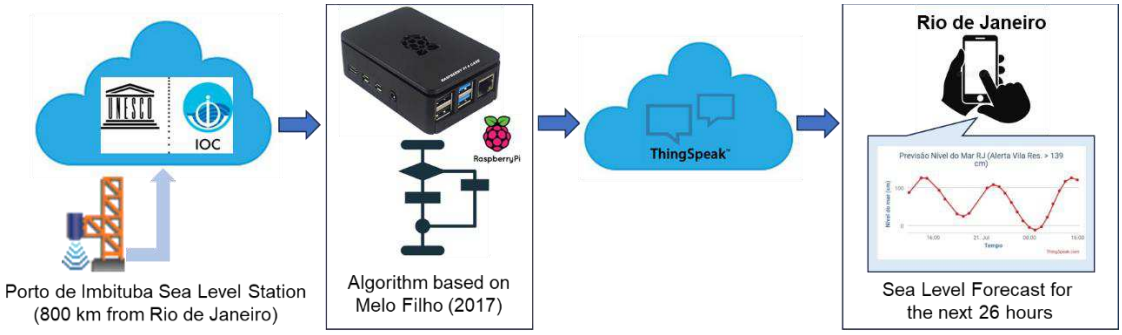


Figure 3: Description of the meteorological tide forecasting system, ranging from sea-level data collection by tide gauges to the display of the meteorological tide forecast on the user interface

The algorithm was divided into five stages. The first stage consisted of near–real-time access to the most recent 30 days of sea-level measurements from the GLOSS station ID 351 (https://www.ioc-sealevelmonitoring.org/station.php?code=imbi), Porto de Imbituba (lat.: −28.2311, lon.: −48.6506), Santa Catarina, Brazil, located approximately 800 km south of Rio de Janeiro (Figure 1). Near real-time data are automatically retrieved via the internet from the database of the Permanent Service for Mean Sea Level (PSMSL), maintained by the Global Sea Level Observing System (GLOSS), a component of the Global Ocean Observing System (GOOS/UNESCO–IOC)[44].

GLOSS station ID 351 is locally operated by the Brazilian Institute of Geography and Statistics (Instituto Brasileiro de Geografia e Estatística - IBGE), under the station code EMMIMB[45]. The station provides sea-level measurements obtained using a radar sensor and a float gauge with an encoder at 1-minute intervals, which are updated on the GLOSS website every 10 minutes.

The second stage of the algorithm involved decomposing the raw sea-level time series into Astronomical Tide (AT), Seasonal Band (SB: 30–365 days), and meteorological tide (MT: 3–30 days) components. Astronomical tide predictions were obtained through harmonic analysis of one year of sea-level data (May 2022 to May 2023) from Imbituba, Santa Catarina. The harmonic constants were computed using routines available in the *ttide* Python library, which is a direct conversion of the *T_Tide* toolbox for MATLAB developed by Pawlowicz et al.[46].

The SB and MT components were extracted using a Fast Fourier Transform (FFT)–based technique with low-pass filtering, with cutoff frequencies set to 0.033 cycles per day (cpd; 30 days) and 0.33 cpd (3 days), respectively[4].

The third stage addressed the propagation of the meteorological tide signal from the Porto de Imbituba station, Santa Catarina, to the Ilha Fiscal station (F-41: 50140), located in Rio de Janeiro (lat.: −22.8967, lon.: −43.1667). The meteorological tide propagation model developed by Melo[4] is based on a lagged linear correlation (τ_0) between the meteorological tide at Porto de Imbituba, $x(t-\tau_0)$, and that at Ilha Fiscal, $y(t)$:

$$y(t) = \alpha x(t-\tau_o), \quad (1)$$

where, according to Bendat and Piersol[47], the transformation coefficient α can be calculated as follows:

$$\alpha = \rho_{xy}(\tau_o)\frac{\sigma_y}{\sigma_x}, \quad (2)$$

where σ_x and σ_y correspond to the square roots of the mean square values of x and y, respectively, and ρ_{xy} is the normalized cross-covariance function between the two stations. In his study, Melo[4] found a maximum correlation value of 0.928 for a time lag of 26 hours and a transformation coefficient of 0.726, calibrated using historical time series from 2003.

The fourth stage involved reconstructing the sea-level time series at the Ilha Fiscal station for the subsequent 26 hours. To this end, the algorithm combined the local astronomical tide forecast with the meteorological tide predicted by the Melo[4] model (Equation 1). The astronomical tide forecast for the Ilha Fiscal gauge station (ID 50140)[48] was based on harmonic constituents derived from sea-level measurements acquired at 5-minute intervals by a radar sensor between January 2018 and December 2019. This measurement period is the same as that used in the construction of the official tide tables published by the Brazilian Navy[48].

Sea-level data for Ilha Fiscal were obtained directly by email (chm.bndo@marinha.mil.br) from the National Oceanographic Data Bank (Banco Nacional de Dados Oceanográficos - BNDO), maintained by the Brazilian Navy's Directorate of Hydrography and Navigation (DHN). This data is also publicly available on a public GitHub account (https://github.com/Dilello/COFFEWS-

MT/blob/main/IlhaFiscalRadar010116_301023.txt). At this stage, an offset of 72.7 cm was also added so that the reconstructed sea level is referenced to the chart datum (Nível de Redução - NR) of Ilha Fiscal, corresponding to Nautical Chart 1515 of Guanabara Bay, Mocanguê Island, and surrounding areas.

The fifth and final stage of the algorithm consisted of transmitting the forecast via the internet to a free data visualization platform based on the Internet of Things (IoT), known as ThingSpeak™ (Figure 3). Through this freely accessible platform, users can consult sea-level forecasts for Rio de Janeiro with a lead time of up to 26 hours (https://thingspeak.com/channels/2459691).

In the present study, the model proposed by Melo[4] was reanalyzed for the year 2022, a period closer to the flooding monitoring conducted in Vila Residencial. The statistical metrics used for model validation were the root mean square error (RMSE) and the coefficient of determination (R^2).

2.3. Meteorological tide flood level

Meteorological tide flood alert levels were defined based on in situ monitoring of flooding events conducted between 2022 and 2024, combined with a survey of historical records of extreme flooding obtained from the local community and from newspaper archives. Informed consent was obtained from all participants and/or their legal guardians, as applicable. The monitoring program consisted of regular field visits scheduled according to forecasts from the Melo model. During these visits, photographic records were collected along Margaridas, Cravos, and Açucenas Streets. These records were subsequently correlated with sea-level measurements from the Ilha Fiscal tide-gauge station (F-41: 50140). The same procedure was applied to historical photographic records provided by community members or retrieved from archival sources.

The flood warning system was divided into two classes. The first class, referred to as the *flood level*, represents the minimum sea-level threshold at which flooding was observed to begin along Cravos, Margaridas, and Açucenas Streets (Figure 2). The second class, termed the *extreme flood level*, corresponds to the sea level at which flooding reached the interior of houses along these streets and expanded to other areas of Vila Residencial (Figure 2).

The evaluation statistics of the flood severity classifier were computed from the confusion matrix. The matrix was populated using the following terminology: true positive (TP),

false negative (FN), false positive (FP), and true negative (TN). Information on the errors committed by the model in each class was derived from the analysis of precision (Pre) and recall (Rec) metrics:

$$Pre = \frac{VP}{VP + FP} \quad (5)$$

$$Rec = \frac{VP}{VP + FN} \quad (6)$$

Precision (Pre) measures the predictive capability of the model, while recall (Rec) quantifies the model's ability to correctly identify the type of flood alert. Given the possibility that the *Flood Level* and *Extreme Flood Level* classes are highly imbalanced (positive class < 1%) relative to their respective negative classes, the Area Under the Precision–Recall Curve ($AUC - PR$) metric was also included. In this study, $AUC - PR$ was computed as the sum of incremental changes in recall weighted by the corresponding local precision values (P_n):

$$\text{AUC} - \text{PR} = \sum_n (R_n - R_{n-1}) \times P_n \quad (7)$$

3. Results

3.1. Astronomical tide analysis

Harmonic analysis identified 48 harmonic constituents at the Imbituba tide-gauge station (GLOSS ID: 351) and 31 harmonic constituents at the Ilha Fiscal station (DHN ID: 50140), all with signal-to-noise ratios (SNR) greater than 2. The ten constituents with the largest amplitudes are listed in Table 2. Both locations were characterized as having semidiurnal astronomical tides (AT) with diurnal inequality (0.25 < Form Factor < 1.5)[9,p.77].

In the interannual (>365 days) and seasonal (30–365 days) frequency bands, harmonic analysis identified only the annual solar constituent SA (365.18 days) at the Imbituba station, with an amplitude of 0.09 ± 0.05 m (SNR = 3.9). In contrast, no harmonic constituents with regular periodicities between 3 and 30 days were identified at either station.

harmonic constant		Imbituba station (IBGE/GLOSS ID: 351)					Ilha Fiscal station (DHN/BNDO ID: 50140)				
tide	period	amp (m)	amp err (m)	pha (°)	pha err (°)	snr	amp (m)	amp err (m)	pha (°)	pha err (°)	snr
Q1	26.89 h	0.033	0.002	37.3	2.7	4.50E+02	0.037	0.002	236.9	2.6	1.70E+03
O1	25.82 h	0.109	0.002	66.0	0.9	4.40E+03	0.039	0.001	88.2	0.7	5.90E+03
P1	24.07 h	0.021	0.001	112.4	5.6	1.20E+02	0.042	0.002	119.3	4.4	1.60E+02
K1	23.94 h	0.062	0.001	124.2	1.7	1.40E+03	0.042	0.001	154.5	1.7	1.90E+03
N2	12.66 h	0.033	0.001	139.8	2.1	7.30E+02	0.079	0.002	309.3	3.7	1.50E+03
M2	12.42 h	0.146	0.001	49.6	0.5	1.30E+04	0.081	0.002	93.4	0.4	2.70E+04
L2	12.19 h	0.010	0.001	70.6	5.0	1.20E+02	0.082	0.002	296.6	6.2	9.4E+01
S2	12.00 h	0.111	0.001	46.7	0.6	8.10E+03	0.083	0.003	81.7	0.6	5.3E+03
K2	11.97 h	0.035	0.001	35.2	1.8	1.30E+03	0.084	0.002	100.0	1.9	1.30E+03
M3	8.28 h	0.015	0.001	124.1	4.2	2.70E+02	0.121	0.001	23.4	4.1	4.6E+01
M4	6.21 h	0.031	0.001	326.9	2.6	4.70E+02	0.161	0.003	93.6	2.8	3.50E+02

Table 2: The ten harmonic constituents with the largest amplitudes identified at the Imbituba, Santa Catarina - SC, and Ilha Fiscal, Rio de Janeiro - RJ, gauge stations. *amp* denotes amplitude, *amp err* the amplitude error, *pha* the phase, *pha err* the phase error, and *snr* the signal-to-noise ratio.

Table 3 presents the contribution of each sea-level variance band at the Imbituba and Rio de Janeiro locations. More than half of the observed variance at both tide-gauge stations was generated by the astronomical tide. In the case of Rio de Janeiro, the astronomical tide accounted for 81% of the total variance, indicating a stronger dominance compared to Imbituba, where it explained only 55%. However, 19% of the variance observed in Rio de Janeiro was not explained by the harmonic constituents and was therefore classified by the algorithm as non-astronomical tide (NAT).

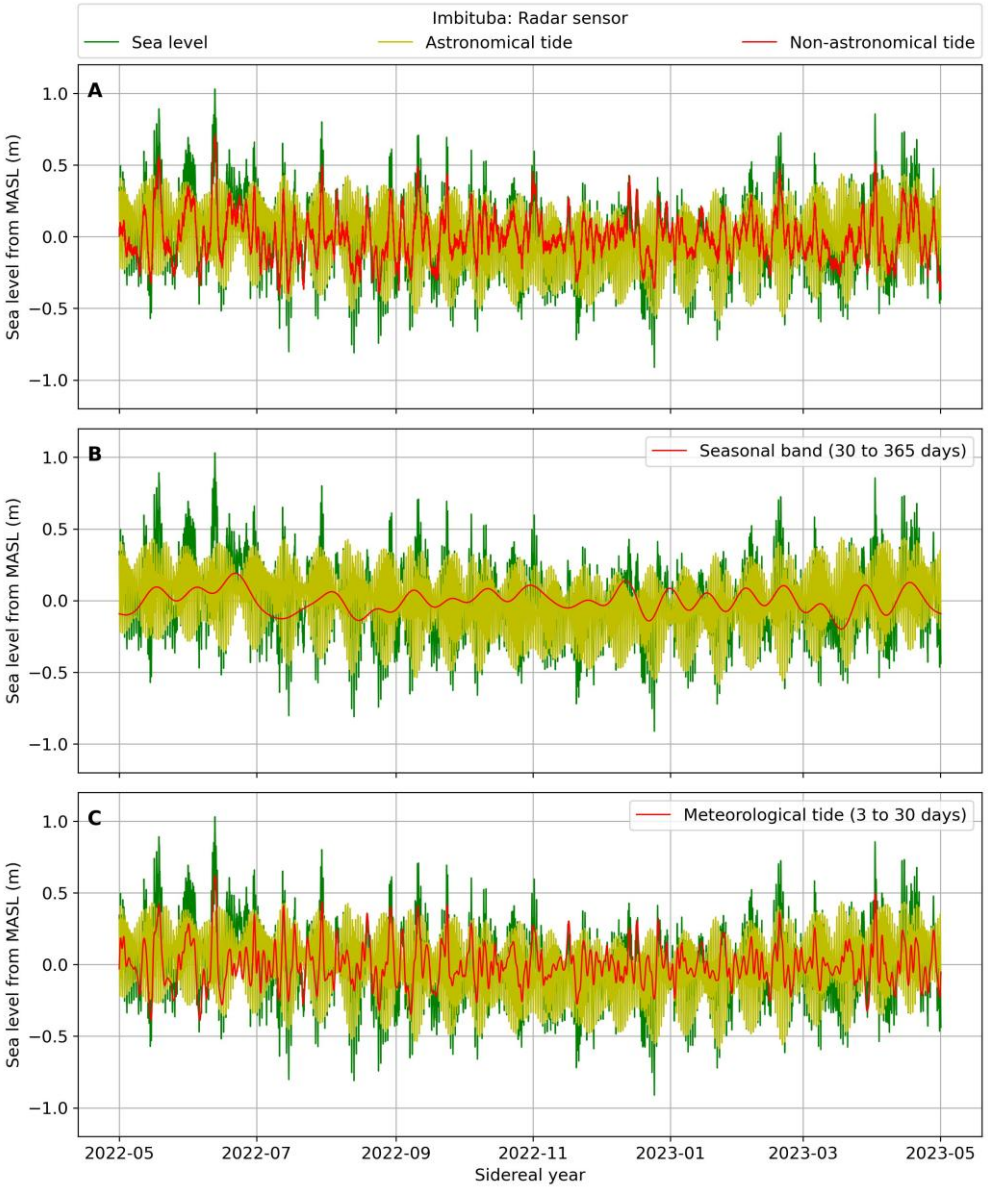
	Sea level	Astronomical tide	Non-Astronomical tide		
			Sazonal band	Meteorological tide	Wind set-up/set-down
Imbituba					
Variance (m²)	6.108	3.406	0.566	2.103	0.044
Sea level percent (%)	100	55.7	9.2	34.4	0.7
Ilha Fiscal					
Variance (m²)	11.462	9.326	0.711	1.456	0.050
Sea level percent (%)	100	81.0	6.1	12.6	0.3

Table 3: Sea-level variance (m²) and percentage (%) associated with the astronomical tide, seasonal band, meteorological tide, and wind set-up/set-down components.

3.2. Non-astronomical tide analysis

At both locations, the FFT procedures implemented in the algorithm identified and extracted from the non-astronomical tide (NAT) the time series corresponding to the seasonal (30–365 days), meteorological (3–30 days), and wind set-up/set-down (2 hours to 3 days) bands (Figures 4 and 5). At Imbituba, the meteorological tide band accounted for 34.4% of the observed variance. In Rio de Janeiro, the variance associated with the meteorological tide band was reduced by approximately half, reaching a value of 12.6% (Table 3).

At both locations, the variance of the seasonal band did not exceed 10%, and the variance associated with the wind set-up/set-down band remained below 1%. As observed for the meteorological tide, both bands exhibit a marked reduction toward Rio de Janeiro.



336

337 Figure 4: Imbituba sea level fluctuation from mean annual sea level (MASL) analysis: A – Non-
338 astronomical tide; B – Seasonal band; and C – Meteorological tide.

339

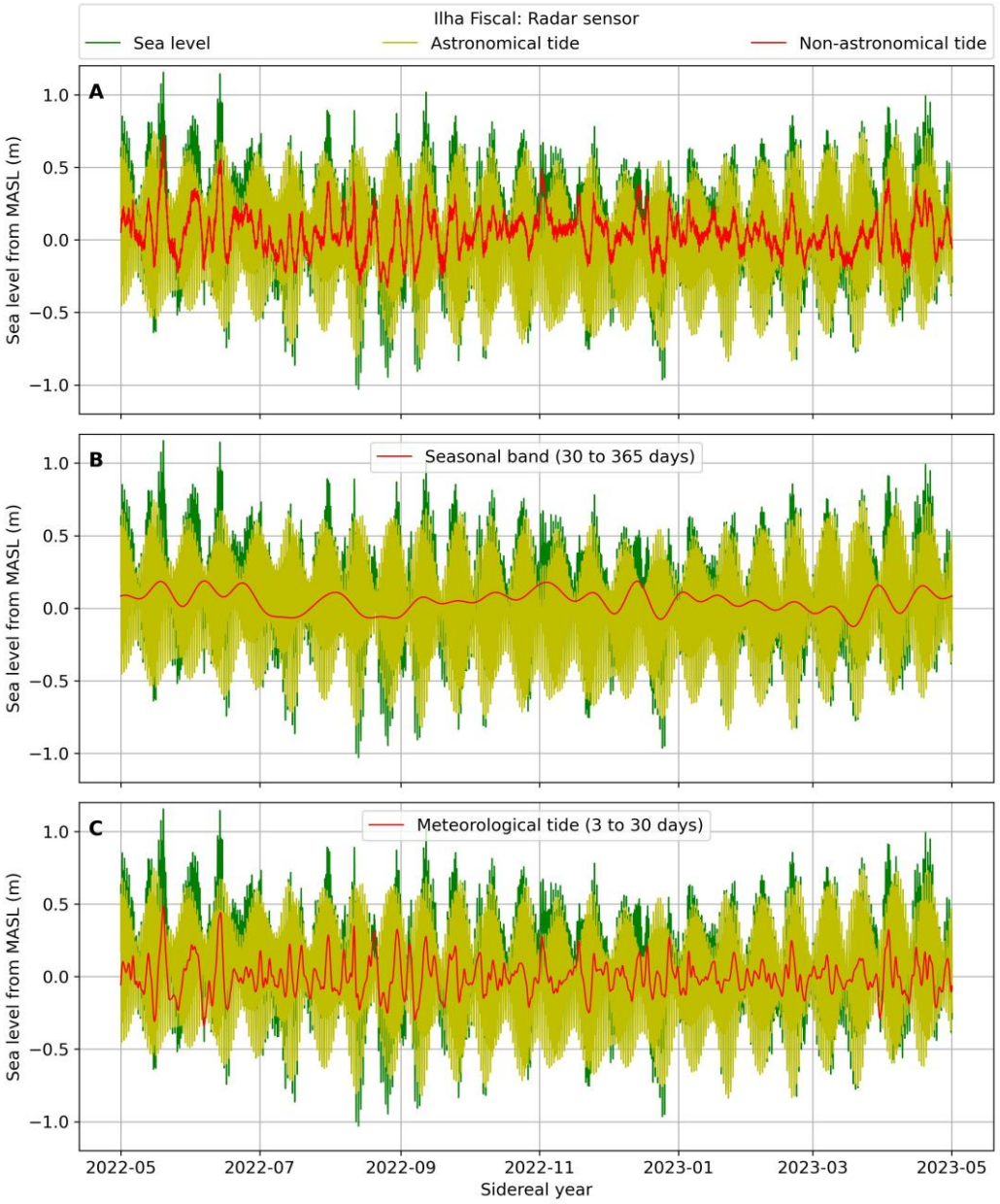


Figure 5: Ilha Fiscal sea level fluctuation from mean annual sea level (MASL) analysis: A - Non-astronomical tide; B – Seasonal band; and C – Meteorological tide.

3.3. Meteorological tide forecast

The comparison between the observed and forecast meteorological tide with a 26-hour lead time over a one-year period is shown in Figure 6. The meteorological tide forecast yielded a root mean square error of only 0.05 m and a coefficient of determination of 0.81, indicating that the model satisfactorily represents meteorological tide variability in Rio de Janeiro (Table 4).

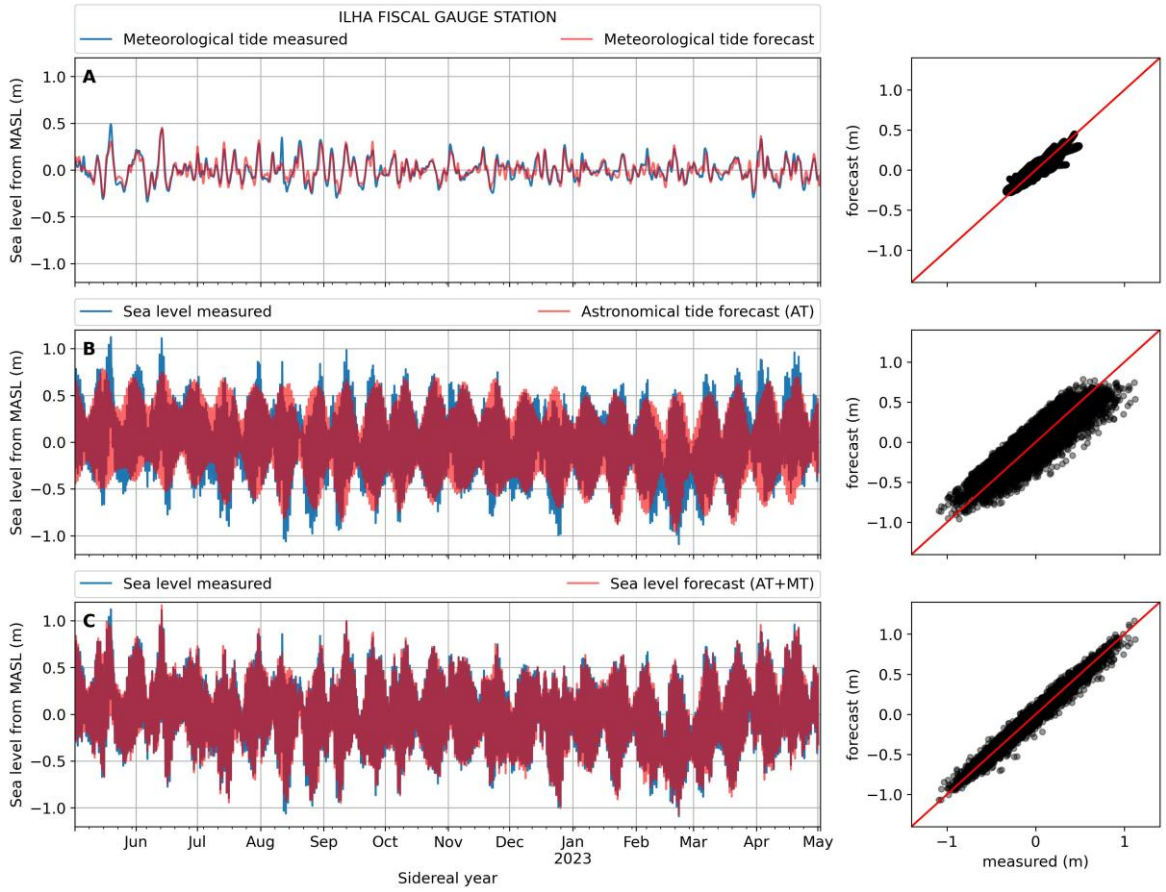


Figure 6: A - Comparison between the observed and forecast meteorological tide; B - Comparison between the observed sea level and the sea level predicted using only the astronomical tide; and C - Comparison between the observed sea level and the sea level predicted by the combined contribution of the astronomical and meteorological tides. MASL denotes mean annual sea level.

ILHA FISCAL GAUGE STATION (May, 2022 to May, 2023)	RMSE	R^2
Meteorological tide model vs. Meteorological tide measured	0.05	0.81
Astronomical tide model (AT) vs. Sea level measured	0.14	0.81
Sea level model (AT+MT) vs. Sea level measured	0.06	0.97

Table 4: Comparison between the forecast and observed sea levels at the Ilha Fiscal gauge station.

3.4. Ilha Fiscal sea level forecast

The sea-level variability forecast for the Ilha Fiscal station over the subsequent 26 hours was reconstructed by combining astronomical and meteorological tide components. The predicted sea level at Ilha Fiscal was compared with the sea-level time series measured at the Ilha Fiscal tide-gauge station (F-41: 50140) (Figure 6). In this comparison, the sea-level forecast based on the Melo[4] model yielded a root mean square error of only 0.06 m and a coefficient of determination of 0.97 (Table 4).

This performance was superior to that obtained using the current sea-level forecasting approach (tide tables), which is based solely on astronomical tide predictions (RMSE: 0.14 m and R^2: 0.81) (Table 4).

3.5. Warning system calibration with field data

The survey of historical photographs (1963–2021) combined with field visits conducted during 2022 and 2023 made it possible to identify flooding events of different magnitudes in the Vila Residencial area. These records allowed the identification of the sea-level thresholds at which flooding begins and when it becomes more severe, with water entering residential buildings (Figure 7).

Flood monitoring indicated that a sea-level elevation of 0.66 m above mean sea level (MSL) marks the onset of flooding, characterized by the initial inundation of streets and stormwater drainage galleries. Historical photographic records further showed that flooding starts to encroach onto sidewalks and residential properties when sea level exceeds 1.0 m above MSL.

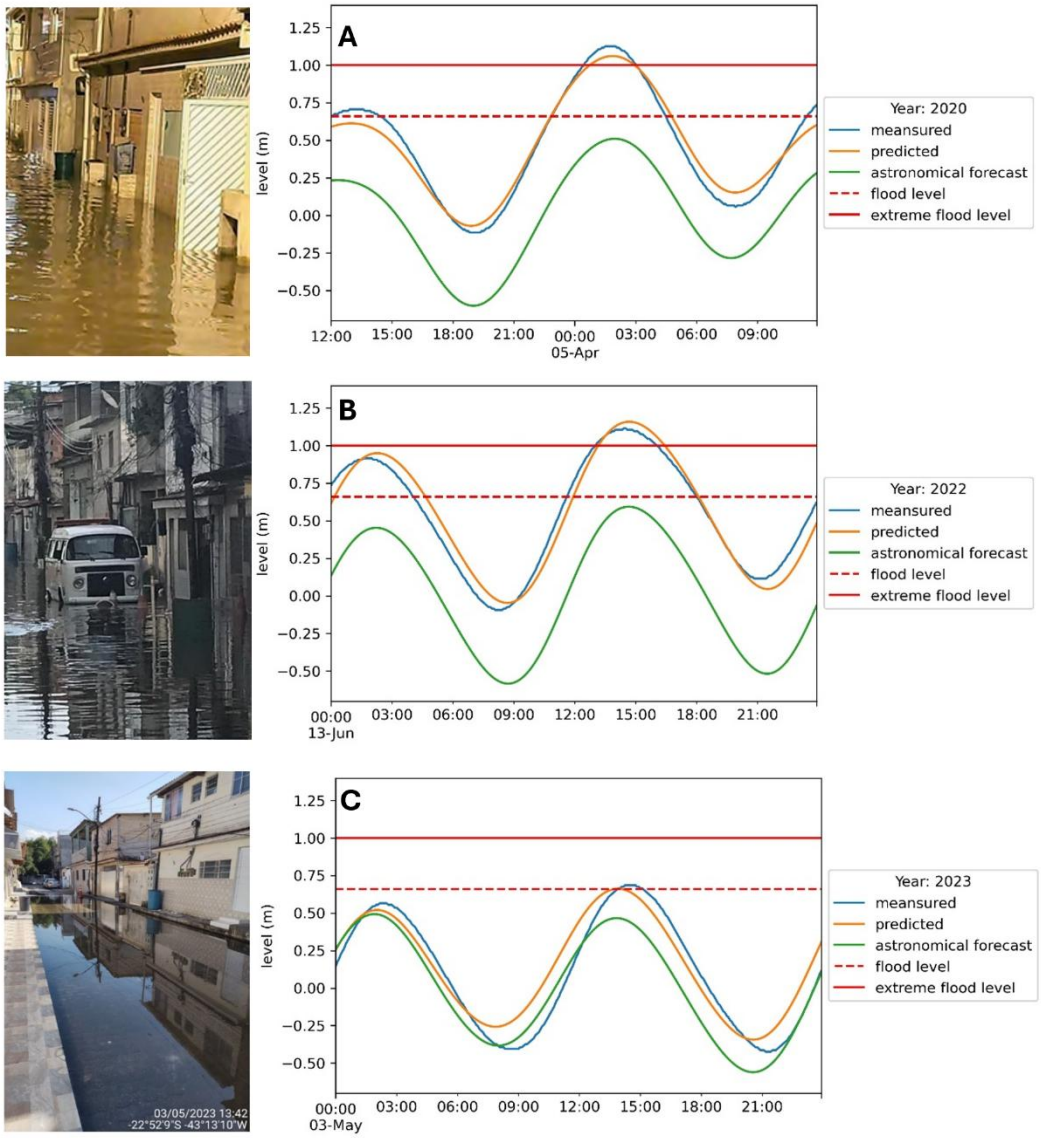


Figure 7: Calibration of the flood alert system based on historical records and in situ flood observations: A – Extreme flood event on 05-April-2020 (by SGCOM/UFRJ); B – Extreme flood event on 13-June-2022 (by Agelio R. Gama); and C – Flood event on 03-May-2023 (by this study during monitoring).

The inclusion of the meteorological tide significantly improved the forecast performance, particularly for the *Flood Alert* class (Table 5). Even though the *Extreme Flood Alert* represents a very rare event (7 cases out of 8,735 samples, ≈ 0.08%), a clear improvement in sea-level prediction was observed when the contribution of the meteorological tide was considered. The AUC–PR proved to be a more reliable metric in situations where the events of interest are rare and the datasets are highly imbalanced, as is the case for the *Extreme Flood Alert*. In contrast, accuracy appeared to be a misleading metric, yielding high values (0.96–1.00) despite limited predictive skill for rare events.

Sea level forecast **without** meteorological tide								
Type warning	Sea level limit (m)	N total	N >Sea level limit	Precision	Recall	F1	ACC	AUC-PR
Flood	0.66	8735	208	0.32	0.55	0.406	0.96	0.18
Extreme flood	1.00	8735	7	0.00	0.00	0.000	1.00	0.00
Sea level forecast **with** meteorological tide								
Type warning	Sea level limit (m)	N total	N >Sea level limit	Precision	Recall	F1	ACC	AUC-PR
Flood	0.66	8735	208	0.67	0.90	0.765	0.99	0.66
Extreme flood	1.00	8735	7	0.40	0.57	0.471	1.00	0.23

Table 5: Performance evaluation of the 26h coastal flooding warning system based on meteorological tide

4. Discussion

The availability of a web-based global sea level station monitoring service providing real-time sea level data from GLOSS tide gauge stations was fundamental to the operational performance of the COFFEWS-MT forecasting model, which critically depends on continuous real-time access to sea level measurements from the Port of Imbituba station (GLOSS ID: 351).

Founded in 1933 at the Liverpool Tidal Institute under the leadership of Joseph Proudman, the Permanent Service for Mean Sea Level (PSMSL) serves as the global data bank for long-term sea level observations from gauges stations[44]. Since 1990, PSMSL has been maintained within the framework of the Global Sea Level Observing System (GLOSS), which was established by the Intergovernmental Oceanographic Commission (IOC) of UNESCO in 1985[49]. GLOSS operates as an Observations Coordination Group (OCG) under the Global Ocean Observing System (GOOS) and the WMO Integrated Global Observing System (WIGOS).

The Flanders Marine Institute (VLIZ, Belgium) currently provides a web-based global sea level station monitoring service that enables real-time visualization and access to tide gauge data. This case study highlights the critical importance of maintaining uninterrupted web-based PSMSL and GLOSS services for the development and operational implementation of low-cost coastal flooding prediction and early warning systems based on meteorological tides.

This type of model, based on correlation between tide gauge stations, highlights the importance of the approximately 1000 km spatial resolution of the PSMSL tide gauge network to ensure the early detection—about one day in advance—of meteorological tides. In this context, we suggest the inclusion of additional real-time tide gauge stations in the PSMSL network along the Brazilian coast, particularly in the municipalities of Rio de Janeiro – RJ and Vitória – ES. Such additions would help prevent the loss of the

meteorological tide signal caused by abrupt variations in continental shelf width and depth between the Tubarão Bay and the Abrolhos Bank regions[23].

The concept of meteorological tide enabled a simple methodological approach while also providing an accessible explanation of the physical processes underlying meteorological tides. This conceptual clarity facilitates communication with vulnerable populations and local authorities. Currently, the municipality of Rio de Janeiro operates a public early warning system for extreme meteorological events, known as AlertaRio (https://www.sistema-alerta-rio.com.br/). However, AlertaRio does not yet provide coastal flooding forecasts driven by meteorological tides for vulnerable communities within the municipality. This limitation is partly related to the limited dissemination and understanding of the meteorological tide phenomenon. In this context, the present case study is expected to raise awareness of the role of meteorological tides in coastal flooding events in Rio de Janeiro and to contribute to a broader set of solutions aimed at strengthening the resilience of vulnerable coastal communities.

The low computational effort required by the meteorological tide predictive model enabled the provision of a free forecasting service through COFFEWS-MT. This feature is particularly desirable, as most communities vulnerable to coastal flooding cannot afford forecasting services based on high–computational-cost numerical modeling. Barbier[50] showed that, in 2000, 95% of the rural population (approximately 59 million people) living in the Low-Elevation Coastal Zone (LECZ) across 15 developing countries (including Brazil) were poor, with living conditions characterized by high infant mortality and malnutrition. This context further reinforces the need for free, accessible solutions capable of reaching the most vulnerable segments of the LECZ population.

The risk of flooding from meteorological tides may be affecting several other coastal communities around the world, as variations in the continental shelf level associated with Kelvin waves, Continental Shelf Waves, and Coastal Trapped Waves have been detected in various regions, such as the coast of Australia[51–53], South Africa[54,55], and the west coast of the Americas[56,57]. Potentially, a forecasting system could be applied in these regions, as long as there is a network of tide gauges between the meteorological tide generating area and the affected area.

The development and validation of the COFFEWS-MT directly contribute to UN Decade Challenge 6: Enhancing community resilience to ocean hazards, particularly through the

advancement of People-Centred Early Warning Systems for ocean-related hazards based on predictive modelling[58]. Its relevance extends to policymakers, scientists, and coastal communities by fostering collaboration aimed at strengthening coastal resilience.

Prior to this study, the Vila Residencial community relied exclusively on physical protection measures such as dikes, walls, and hydraulic gates, constructed through community-organized and self-funded collective efforts (Figure 8). In this context, the CFFWS-MT emerges as an additional and complementary tool to enhance the coastal resilience of this community.



Figure 8: A – Hydraulic gate blocking the inflow of seawater (left) into the urban drainage system of Margaridas Street (right); B – Final connection of the Margaridas Street urban drainage system to the sea.

5. Conclusions

This study demonstrated the performance of a low-cost and freely accessible coastal flooding forecasting system based on meteorological tide, providing up to 26 hours of lead time for a vulnerable community in Rio de Janeiro. During the reanalysis for the year 2022, the model proposed by Melo[4] showed performance comparable to its original validation period (2003).

Field monitoring of flooding events combined with the analysis of historical records enabled the determination of flood and extreme flood thresholds used in the early warning system. The coastal flooding forecasting system based on meteorological tide showed a significant improvement in sea level prediction during flooding events when compared to forecasts based solely on astronomical tide.

The low computational cost and straightforward implementation of the proposed approach represent its main advantages over conventional numerical models, particularly when the target audience is highly vulnerable coastal populations.

6. Funding Declaration

The authors acknowledge the Coordenação de Aperfeiçoamento de Pessoal de Nível Superior - Brasil (CAPES) for financial support and for funding the article processing charges (APC).

References

1. Haasnoot, M.; Winter, G.; Brown, S.; Dawson, R. J.; Ward, P. J.; Eilander, D. (2021) Long-term sea-level rise necessitates a commitment to adaptation: a first order assessment. **Climate Risk Management**, 34, doi:10.1016/j. crm.2021.100355.

2. Oppenheimer, M.; Glavovic , B. C.; Hinkel, J.; van de Wal, R.; Magnan, A.K. *et al*. (2019) **Sea Level Rise and Implications for Low-Lying Islands, Coasts and Communities**. In: IPCC Special Report on the Ocean and Cryosphere in a Changing Climate [Pörtner, H.-O; Roberts, D.C.; Masson-Delmotte, V.; Zhai, P.; Tignor, M. *et al.* (eds.)]. Cambridge University Press, Cambridge, UK and New York, NY, USA, pp. 321–445. https://doi.org/10.1017/9781009157964.006

3. Glavovic, B.C.; Dawson, R.; Chow, W.; Garschagen, M.; Haasnoot, M. et al. (2022) **Cross-Chapter Paper 2: Cities and Settlements by the Sea.** In: Climate Change 2022: Impacts, Adaptation and Vulnerability. Contribution of Working Group II to the Sixth Assessment Report of the Intergovernmental Panel on Climate Change [Pörtner, H.-O.; Roberts, D.C.; Tignor, M.; Poloczanska, E.S.; Mintenbeck, K. *et al*. (eds.)]. Cambridge University Press, Cambridge, UK and New York, NY, USA, pp. 2163–2194, doi: 10.1017/9781009325844.019

4. Melo, E. (2017) **Maré meteorológica na Costa Brasileira**. Tese Professor Titular, Escola de Engenharia, Universidade Federal de Rio Grande. 328 p. Available in Portuguese at http://repositorio.furg.br/handle/1/7212

5. Kirezci, E.; Young, I. R.; Ranasinghe, R.; Muis, S.; Nicholls, R. J. *et al.* (2020) Projections of global-scale extreme sea levels and resulting episodic coastal flooding over the 21st Century. **Nature. Scientific Reports** 10, 11629. https://doi.org/10.1038/s41598-020-67736-6

6. Neves, S. da C. (1992) **Variação da maré meteorológica no litoral sudeste do Brasil: 1965 – 1986**. Tese (Doutorado), Programa de Pós-graduação em Engenharia Oceânica, COPPE, Universidade Federal do Rio de Janeiro. 113 p. Available in Portuguese at https://w1files.solucaoatrio.net.br/atrio/ufrj-peno_upl/THESIS/10002498/1992_mestrado_sebastiao_da_costa_neves_filho_20211129173240 97.pdf

7. Marone, E.; Camargo, R. de (1994) Marés meteorológicas no litoral do Estado do Paraná: O evento de 18 de agosto de 1993. **Nerítica**,8, pp.73-85. DOI: https://doi.org/10.5380/rn.v8i1-2.85081

8. Bowden, K. F. (1983) **Physical Oceanography in Coastal Waters**, Ellis Horwood Ltd., Great Britain, 302 p.

9. Pugh D.; Woodworth, P. (2014) **Sea-Level Science. Understanding Tides, Surges Tsunamis and Mean Sea Level**. Cambridge University Press, New York. 395 p.

10. Dean, R. G.; Dalrymple, R. A. (2000) **Water wave mechanics for engineers and scientistis**. Advanced Series on Ocean Engineering – Volume 2. World Scientific, Singapore, 353 p.

11. Flather, R. A. (2001) Storm Surges. In: **Encyclopedia of Ocean Sciences**. Edited by Steele, J. H.; Turekian, K. K.; Thorpe, S.A., p. 2882-2892.

12. Freeman, J. C.; Baer, L.; Jung, G. H. (1957) Bathystrophic Storm Tide**. Journal of Marine Research**, 16, 1, p.12-22. https://elischolar.library.yale.edu/journal_of_marine_research/878/

13. Woodworth, P.L.; Melet, A.; Marcos, M. *et al.* (2019) Forcing Factors Affecting Sea Level Changes at the Coast. **Surveys Geophysics**, 40, pp. 1351–1397 https://doi.org/10.1007/s10712-019-09531-1

14. Huthnance, J. M. (2001) Coastal Trapped Waves. In: **Encyclopedia of Ocean Sciences**. Edited by Steele, J. H.; Turekian, K. K.; Thorpe, S. A., p. 443-450.

15. Hughes, C. W.; Fukumori, I.; Griffies, S. M.; Huthnance, J. M.; Minobe, S. **et al**. (2019) Sea Level and the Role of Coastal Trapped Waves in Mediating the Influence of the Open Ocean on the Coast. **Surveys in Geophysics**, 40, pp. 1467-1492. DOI: https://doi.org/10.1007/s10712-019-09535-x

16. Gönnert, G.; Dube, S. K.; Murty, T.; Siefert, W. (2001) Global Storm Surges: Theory, Observations and Applications. **Die Küste**, 63, 623 p.

17. World Meteorological Organization (2011) **Guide to Storm Surge Forecasting.** WMO Report No. 1076. Geneva: World Meteorological Organization. https://library.wmo.int. Accessed 2 July 2026

18. Castro, B. M.; Lee, T. N. (1995) Wind-forced Sea Level Variability on the Southeast Brazilian Shelf. **Journal of Geophysical Research**, V. 100, C8, pp. 16045-16056. DOI: https://doi.org/10.1029/95JC01499

19. Stech, J. A.; Lorenzzetti, J. A. (1992) The Response of the South Brazil Bight to Wintertime Cold Fronts. **Journal of Geophysical Research**, V. 97, No. C6, pp. 9507-9520 https://doi.org/10.1029/92JC00486

20. Camargo, R.; Harari, J.; Lopes, R.; Caruzzo, A.; Zacharias, D. C. (2000) Implementação de Sistema de Previsão de Marés Meteorológicas no Atlântico Sudoeste. In: **XI Congresso Brasileiro de Meteorologia**, Rio de Janeiro. Anais, p 2646-2654. Available in Portuguese at ResearchGate: https://www.researchgate.net/publication/295548664_Implementacao_de_sistema_de_previsao_de_mares_meteorologicas_no_Atlantico_Sudoeste . Last acessed at 07-21-2026.

21. Camargo, R.; Harari, J.; Biscaro, T. S.; Biazet, B. (2002) Avaliação das Previsões de Maré Meteorológica realizadas com o Princeton Ocean Model no Laboratório Master/IAG/USP. **XII Congresso Brasileiro de Meteorologia**, Foz de Iguaçu-PR, Anais, p. 2022-2028

22. França, B. R. L. (2013) **Ondas Costeiras Confinadas na Plataforma Continental Sul-Sudeste do Brasil**. Dissertação (Mestrado), Programa de Pós-Graduação em Engenharia Oceânica, COPPE, Universidade Federal do Rio de Janeiro, RJ, Brasil, 77 p. https://w1files.solucaoatrio.net.br/atrio/ufrj-peno_upl//THESIS/6000264/2013_mestrando_bruna_reis_leite_franca_20200405213423662.pdf

23. Freitas, P. P. de; Paiva, A. de M.; Cirano, M.; Mill, G. N.; Costa, V. S. da; Gabioux M., França, B. R. L. (2021) Coastal trapped waves propagation along the Southwestern.

562 Atlantic Continental Shelf. **Continental Shelf Research**, 226, 104496, 17 p. DOI:
563 https://doi.org/10.1016/j.csr.2021.104496

564 24. Santoro, P.; Fernández, M.; Fossati, M.; Cazes, G.; Terra, R.; Piedra-Cueva, I. (2011)
565 Pre-operational forecasting of sea level height for the Río de la Plata. **Applied**
566 **Mathematical Modelling**, 35, 5, pp. 2462-2478
567 https://doi.org/10.1016/j.apm.2010.11.065

568 25. Truccolo, E. C. (1998) **Maré Meteorológica e Forçantes Atmosféricas Locais em**
569 **São Francisco do Sul - SC**. Dissertação (Mestrado), Programa de Pós-Graduação em
570 Engenharia Ambiental, Universidade Federal de Santa Catarina, SC, Brasil.
571 http://repositorio.ufsc.br/xmlui/handle/123456789/77725

572 26. Truccolo, E.C.; Franco, D.; Schettini, C. A. F. (2004) The Low Frequency Sea Level
573 Oscillations in the Northern Coast of Santa Catarina, Brazil. **Journal of Coastal**
574 **Research**, SI 39, pp. 547-552. http://www.jstor.org/stable/25741633 Accessed 22 July
575 2026.

576 27. Oliveira, M. M. F. de (2004) **Redes Neurais Artificiais na Predição da Maré**
577 **Meteorológica em Paranaguá - PR**, Dissertação (Mestrado), Programa de Pós-
578 Graduação em Engenharia Civil, COPPE, Universidade Federal do Rio de Janeiro, RJ,
579 Brasil, 149 p. Available in Portuguese at https://coc.ufrj.br/lista-dissertacao-de-
580 mestrado/redes-neurais-artificiais-na-predicao-da-mare-meteorologica-em-paranagua-
581 pr/

582 28. Oliveira, M. M. F. de; Ebecken, N. F. F.; Santos, I. de A. Neves, C. F.; Caloba, L. P.;
583 Oliveira, J. L. F. de (2006) Modelagem da Maré Meteorológica utilizando Redes Neurais
584 Artificiais: uma Aplicação para a Baía de Paranaguá – PR, Parte 1: Dados Meteorológicos
585 da Estação de Superfície, **Revista Brasileira de Meteorologia**, v. 21, n. 2, pp. 220 231,
586 2006.

587 29. Oliveira, M. M. F. de; Ebecken, N. F. F.; Santos, I. de A. Neves, C. F.; Caloba, L. P.;
588 Oliveira, J. L. F. de (2007) Modelagem da Maré Meteorológica utilizando Redes Neurais
589 Artificiais: uma Aplicação para a Baía de Paranaguá – PR, Parte 2: Dados de Reanálise
590 do NCEP/NCAR, **Revista Brasileira de Meteorologia**, v. 23, n. 1, pp. 53-62, 2007.
591 https://doi.org/10.1590/S0102-77862007000100006

30. Oliveira, M. M. F. de (2009) **Análise Estatística de Dados Ambientais com Aplicação da Teoria de Valores Extremos e Predição do Nível do Mar utilizando Redes Neurais Artificiais** Tese (Doutorado), Programa de Pós-Graduação em Engenharia Civil, COPPE, Universidade Federal do Rio de Janeiro, RJ, Brasil, 253 p. Available in Poruguese at https://coc.ufrj.br/lista-teses-de-doutorado/analise-estatistica-de-dados-ambientais-com-aplicacao-da-teoria-de-valores-extremos-e-predicao-do-nivel-do-mar-utilizando-redes-neurais-artificiais/

31. Gill, A. E. (1982) **Atmosphere-Ocean Dynamics.** International Geophysics Series, Academic Press, 662 p. https://www.sciencedirect.com/bookseries/international-geophysics/vol/30/suppl/C

32. Wunsch C.; Stammer D. (1997) Atmospheric loading and the oceanic 'inverted barometer' effect. **Reviews of Geophysics**, 35,1, pp. 79-107 https://doi.org/10.1029/96RG03037

33. Hamon, B. V. (1962) The spectrums of mean sea level at Sydney, Coffs Harbour, and Lord Howe Island. **Journal of Geophysical Research**, 67, pp. 5147-5155. DOI: https://doi.org/10.1029/JZ067i013p05147

34. Hamon, B. V. (1966) Continental shelf waves and the effects of atmospheric pressure and wind stress on sea level. **Journal of Geophysical Research**, 71, pp. 2883—2896. DOI: https://doi.org/10.1029/JZ071i012p02883

35. Hamon, B. V.; Hannan, E. J. (1963) Estimating relations between time series. **Journal of Geophysical Research**, 68, pp. 6033-6041. DOI: https://doi.org/10.1029/JZ068i021p06033

36. Adams J. K.; Buchwald V. T. (1969) The generation of continental shelf waves. **Journal of Fluid Mechanical**, 35, 4, pp. 815-826. DOI: https://doi.org/10.1017/S0022112069001455

37. Mysak, L. A. (1967) On the theory of continental shelf waves. **Journal of Marine Research**, 25,3, pp. 205 - 227. https://elischolar.library.yale.edu/journal_of_marine_research/1100

38. Filippo, A.; Kjerfve, B.; Torres Júnior, A. R.; Fernandes, A. M.; (2012) Low-frequency variability of sea level along the mid-atlantic coast of south America. **Revista Brasileira de Geofísica**, 30, 5–14.

https://www.researchgate.net/publication/257881096_Low-frequency_variability_of_sea_level_along_the_Mid-Atlantic_Coast_of_South_America_in_1983

39. Gan, M. A.; Rao, V. B. (1991) Surface cyclogenesis over South America. **Monthly Weather Review**, 119: 1293‑1302. DOI: https://doi.org/10.1175/1520-0493(1991)119%3C1293:SCOSA%3E2.0.CO;2

40. Gramcianinov, C. B.; Campos, R. M.; de Camargo R.; Hodges K. I.; Guedes Soares C.; da Silva Dia, P. (2020). Analysis of Atlantic extratropical storm tracks characteristics in 41 years of ERA5 and CFSR/CFSv2 databases. **Ocean Engineering**, 216: 108111. https://doi.org/10.1016/j.oceaneng.2020.108111

41. Destéfani, B. A. O.; Broggio, M. F.; Garcia, C. A. E. (2025) Climatological Study on Cyclone Genesis and Tracks in Southern Brazil from 1979 to 2019. **Atmosphere**, 16: 92. https://doi.org/10.3390/atmos16010092

42. Jantsch, M. (2024). **Climatologia de ciclones extratropicais e ressacas na costa sul e sudeste do brasil entre 1979 e 2020**. Tese de Doutorado. Pós-Graduação em Geografia do Instituto de Geociências da Universidade Federal do Rio Grande do Sul. Porto Alegre. 165 p. https://lume.ufrgs.br/handle/10183/280787

43. Barbosa, G. S.; Drach, P.; Rossi, A. M. G. *et al*. (2016) **Diagnóstico da Vila Residencial da UFRJ. Relatório Final – Diagnóstico Vila Residencial da UFRJ**. Extensão Universitária – PR5. Rio de Janeiro. 62 p. Available in Portuguese at ResearchGate: https://www.researchgate.net/publication/321034568_DIAGNOSTICO_DA_VILA_RESIDENCIAL_DA_UFRJ_Extensao_Universitaria-PR5_Rio_de_Janeiro-2016_RELATORIO_FINAL-DIAGNOSTICO_VILA_RESIDENCIAL_DA_UFRJ. Last acessed at 07-21-2026.

44. Holgate, S.J.; Matthews, A.; Woodworth, P.L.; Rickards, L.J.; Tamisiea, M.E. *et al*. (2013) New data systems and products at the Permanent Service for Mean Sea Level. **Journal of Coastal Research**, 29(3), 493–504. DOI: https://doi.org/10.2112/JCOASTRES-D-12-00175.1

45. Instituto Brasileiro de Geografia e Estatística (2022) **Relatório descritivo de estação maregráfica**. Estação IMBITUBA – SC, ID: EMMIMB. Instituto Brasileiro de

Geografia e Estatística – IBGE. 3 p. Available in Portuguese at https://www.ibge.gov.br/geociencias/informacoes-sobre-posicionamento-geodesico/rede-geodesica/10842-rmpg-rede-maregrafica-permanente-para-geodesia.html?=&t=relatorio-descritivo-de-estacao-maregraficarmpg

46. Pawlowicz, R.; Beardsley, B.; Lentz, S. (2002) Classical tidal harmonic analysis including error estimates in MATLAB using T_TIDE. **Computers & Geosciences**, 28, 8, pp. 929-937. DOI: https://doi.org/10.1016/S0098-3004(02)00013-4

47. Bendat, J. S.; Piersol, A.G. (1999). **Measurement and Analysis of Random Data**. Ed. Wiley. 390 p.

48. Diretoria de Hidrografia e Navegação (2021) **Descrição de estação maregráfica.** F41 - Padrão - ILHA FISCAL - 50140 - Versão 1/2021. Diretoria de Hidrografia e Navegação – DHN, Marinha do Brasil, 2 p.

49. Global Sea-Level Observing System (2012) **Global Sea-Level Observing System (GLOSS). Implementation Plan – 2012**. UNESCO/IOC, IOC Technical Series No.100, Paris, 41 p. https://unesdoc.unesco.org/ark:/48223/pf0000217832

50. Barbier, E. B. (2015) Climate change impacts on rural poverty in low-elevation coastal zones. **Estuarine, Coastal and Shelf Science**, 165, pp. A1-A13. DOI: https://doi.org/10.1016/j.ecss.2015.05.035

51. Freeland, H.J.; Boland, F.M.; Church, J.A.; Clarke A.J.; Forbes, A.M.G.; Huyer, A.; Thompson, R.O.R.Y.; White, H.J. (1986) The Australian Coastal Experiment: A Search for Coastal-Trapped Waves. **Journal of Physical Oceanography**, V. 16, p. 1230-1249. DOI: https://doi.org/10.1175/1520-0485(1986)016<1230:TACEAS>2.0.CO;2

52. Church, J.A.; Freeland, H.J.; Smith, R.L. (1986a) Coastal-Trapped Waves on the East Australian Continental Shelf, Part I: Propagation of Modes. **Journal of Physical Oceanography**, V. 16, p. 1229-1943. DOI: https://doi.org/10.1175/1520-0485(1986)016<1929:CTWOTE>2.0.CO;2

53. Church, J.A.; White, N.J.; Clarke, A.J.; Freeland, H.J.; Smith, R.L. (1986b) Coastal-Trapped Waves on the East Australian Continental Shelf, Part II: Model Verification. **Journal of Physical Oceanography**, V. 16, p. 1245-1957. DOI: https://doi.org/10.1175/1520-0485(1986)016<1945:CTWOTE>2.0.CO;2

684 54. Schumann, E.H.; Brink, K.H. (1990) Coastal-Trapped Waves off the Coast of South
685 Africa: Generation, Propagation and Current Structures. **Journal of Physical**
686 **Oceanography**. V.20, p.1206-1218. https://doi.org/10.1175/1520-
687 0485(1990)020<1206:CTWOTC>2.0.CO;2

688 55. Cuevas, B.A.; Brundrit, G.B.; Shipley, A.M. (1986) Low-Frequency Sea-level
689 Fluctuations along the Coasts of Namibia and South Africa. **Geophysical Journal of the**
690 **Royal Astronomical Society**. V.87, p. 33-42, 1986. DOI:

691 56. Brink, K.H. (1982) A Comparison of Long Coastal Trapped Waves with Observations
692 off Peru. Journal of Physical Oceanography, V. 12, p. 897-913. DOI:
693 https://doi.org/10.1175/1520-0485(1982)012<0897:ACOLCT>2.0.CO;2

694 57. Enfield, D.B.; Allen, J.S. (1983) The Generation and Propagation of Sea Level
695 Variability Along the Pacific Coast of Mexico. **Journal of Physical Oceanography**, V.
696 13, p. 1012-1033, 1983. DOI: https://doi.org/10.1175/1520-
697 0485(1983)013<1012:TGAPOS>2.0.CO;2

698 58. Pinardi, N.; Kumar, T. S.; Alvarez-Fanjul, E.; Ansong, J. K.; Burgos, A. *et al.* (2024).
699 **Ocean Decade Vision 2030 White Papers – Challenge 6: Increase Community**
700 **Resilience to Ocean Hazards**. Paris, UNESCO IOC. (The Ocean Decade Series, 51.6.).
701 https://doi.org/10.25607/smm1-nq79

Supplementary Files

This is a list of supplementary files associated with this preprint. Click to download.

- BrutoImbi010120070524.txt
- IlhaFiscalRadar010116301023.txt